

WAVELET TRANSFORMS FOR EEG SIGNAL DENOISING AND DECOMPOSITION

Ibtihal Hassan Elshekhdri
Biomedical Engineering Department,
Sudan University of Science and Technology,
Khartoum, Sudan.
hoola88@hotmail.com

Magdi Baker MohamedAmien
Electrical and Electronic Engineering Department,
University of Khartoum,
Khartoum, Sudan.
magdy.baker@uofk.edu

Ahmed Fragoon
Biomedical Engineering Department,
Sudan University of Science and Technology,
Khartoum, Sudan.
ahmedfragoon@sustech.edu

Submitted: Jul, 07, 2023 **Revised:** Sep, 11, 2023 **Accepted:** Sep, 21, 2023

Abstract: EEG signal analysis is difficult because there are so many unwanted impulses from non-cerebral sources. Presently, methods for eliminating noise through selective frequency filtering are afflicted with a notable deprivation of EEG information. Therefore, even if the noise is decreased, the signal's uniqueness should be preserved, and decomposition of the signal should be more accurate for feature extraction in order to facilitate the classification of diseases. This step makes the diagnosis faster. In this study, three types of wavelet transforms were applied: Discrete Wavelet Transform (DWT), Wavelet Packet Transform (WPT), and Stationary Wavelet Transform (SWT), with three mother functions: Haar, Symlet2, and Coiflet2. Three parameters were used to evaluate the performance: Signal-to-Noise Ratio (SNR), Mean Square Error (MSE), and Peak Signal-to-Noise Ratio (PSNR). Most of the higher values of SNR and PSNR were 27.3189 and 40.019, respectively, and the lowest value of MSE was 5.0853 when using Symlet2-SWT level four. To decompose the signal, we relied on the best filter used in the denoising process and applied four methods: DWT, Maximal Overlap DWTs (MODWT), Empirical Mode Decomposition (EMD), and Variational Mode Decomposition (VMD). The comparison has been made between the four methods based on three metrics: energy, correlation coefficient, and distances between the Power Spectral Density (PSD), where the highest value of energy was 5.09E+08 and the lowest value of the PSD was -1.2596 when using EMD.

Keywords: Wavelet transform, mother wavelet, empirical mode decomposition, variational mode decomposition.

I. INTRODUCTION

The ElectroEncephaloGraphy (EEG) is a non-invasive degree of the electrical interest of the mind thru the location of electrodes at the scalp in regions of the mind, and used as the primary sign to pick out an expansion of brain-related conditions, inclusive of narcolepsy, Sleep apnea syndrome, Insomnia, Parasomnia, and Epileptic seizures. There are two origins of the artifacts that impact the EEG signal, namely physiological and non-physiological. The physiological origins consist of ElectroOculoGraphy (EOG) artifacts, ocular artifacts; muscular noise in ElectroMyoGraphy (EMG), cardiac signals, whilst non-physiological factors encompass line disruptions and electrode interference Therefore, removing noise from the EEG signal is of utmost importance during the preprocessing phase. Additionally, decomposition of the EEG signal performs a good function in feature extraction for the classification of epileptic seizures.

When recording EEG data, it is important to be aware of signal artifacts as they can greatly affect the quality of the data. These artifacts have the potential to contaminate the EEG data and must be addressed in order to ensure accurate results. Artifacts refer to undesirable signals that primarily stem from outside of the body like environmental, and inside of the body like ocular, muscle, and cardiac artifacts that produce notable distortions in EEG recordings originate from the body itself [1]. Muscle artifacts are another origin of artifacts. The electrical signals produced by the muscles when they contract can be detected on the surface of the body by means of the EMG technique [2]. This type of artifact may arise from actions such as swallowing, chewing, grimacing, frowning, talking and hiccupping, both during wakefulness and sleep. In addition, the activity of the heart can also generate artifacts in the EEG signal. Depending on the location of the electrodes and the shape of the body, the electrical signals produced by the heart (as reflected in the ECG) may interfere with the EEG [3].

Denosing and decomposition of the EEG signal have been proposed using multiple techniques. The wavelet is the best method for denosing than others in [4]. A numerous noise elimination technique from EEG signal is studied in [5], and the best result was obtained when using WPT. The efficacy of denosing techniques based on wavelets for EEG signals has been investigated in a study on EEG signals [6]. Four distinct discrete wavelet functions were employed to eliminate noise from the Electroencephalogram signal obtained from two different patient groups (healthy and epileptic) to demonstrate the efficiency of DWT in eliminating EEG noise.

IIR low pass filter, FIR low pass and wavelet transform method were applied to the distorted EEG signal; the mother wavelet (symlet) has been more compatible with the EEG signal founded by determining the higher SNR and minimum MSE than the all other filters and wavelets in [7]. Wavelet transform with different kinds of filters such as db2, db4, coif2, coif4, sym2, and sym4 are used to decompose the signal into low and high frequency components in [8]. It is observed that minimax threshold estimation with soft thresholding using the wavelet filter coif4 performs better in terms of PSNR. Various wavelet transform based denosing techniques were discussed in [9]. Several methods have presented the decomposition of a signal, and a comparative study between DWT and maximal overlap DWT for testing stationarity was described in [10]. EMD and VMD and its comparison was made between them in [11]. In [12], a comparison between EMD and Intrinsic timescale decomposition (ITD) was provided.

II. METHODS AND MATERIALS

To achieve the goals of this study, at first, a dataset from the University of Bonn has been used. Secondly, the signal has been denoised in three scenarios. In scenario one, the DWT was used with different mother functions, including Haar, Symlet2, and Coiflet2. In scenario two, the WPT was applied using the same mother functions that were employed in scenario one. In scenario three, a SWT was utilized with the same mother functions that were employed in scenario one, then the three scenarios have been evaluated by three parameters: SNR, MSE, and PSNR. In step three, the signal has been decomposed using four approaches. In approach one, a DWT was applied, in approach two, a maximal overlap DWT was applied. In approach three, the EMD was applied. In approach four, the VMD was applied, then the four approaches have been compared using three parameters: energy, correlation, and distances between the power spectral densities. The schematic representation of the suggested approach is illustrated in Figure 1.

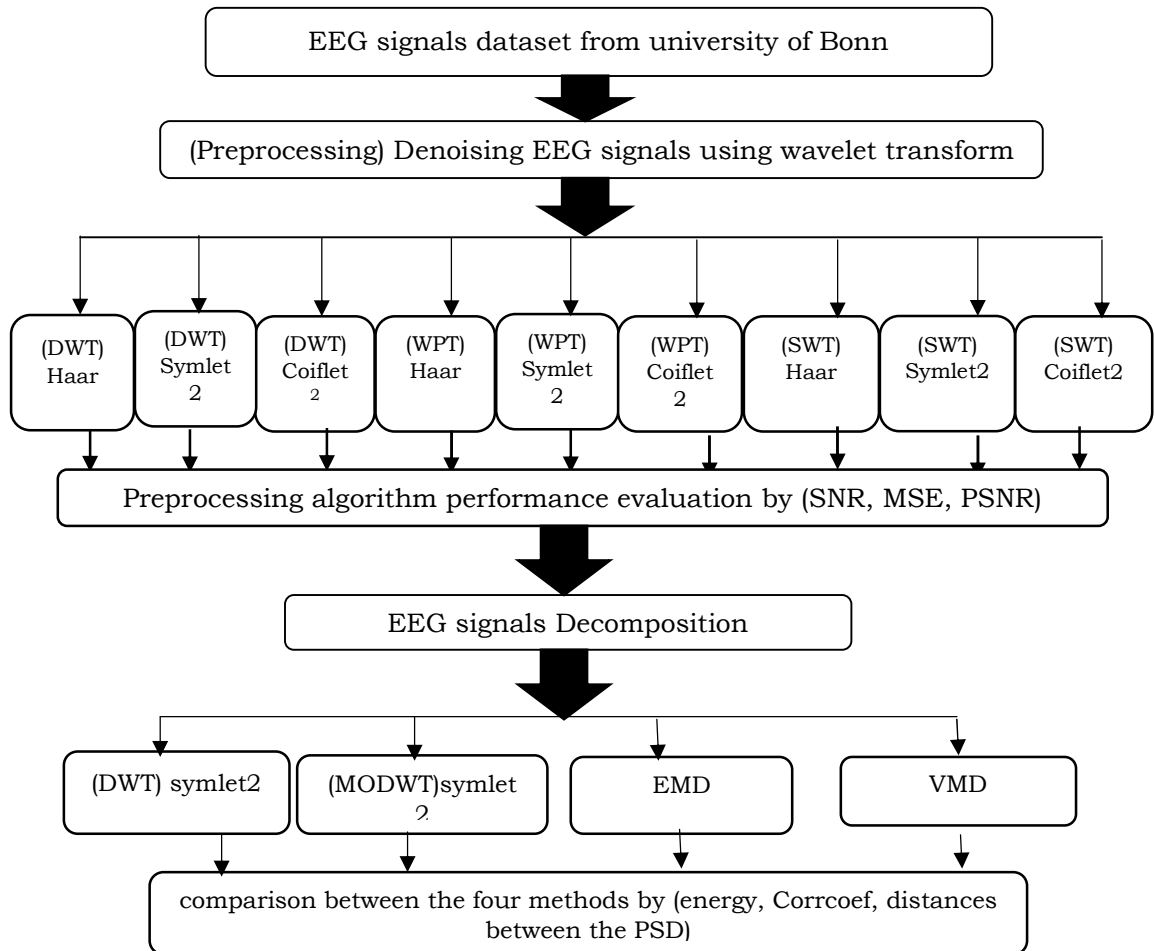


Fig. 1 diagram of the proposal method

A. Dataset

The University of Bonn's publicly available benchmark database was used in this study [13]. The database consists of five subsets (A, B, C, D, and E), the sampling rate of the EEG data is 173.61 Hz, and each of them has a duration of 23.6 s (4096 samples), recorded using a 12-bit resolution, while the spectral bandwidth is 0.5 to 86.8 Hz. A total of 500 EEG epochs belonging to three categories: healthy open and close eyes respectively (A, B), seizure (E), and seizure free (C, D), shown in Figures 2 and 3, respectively.

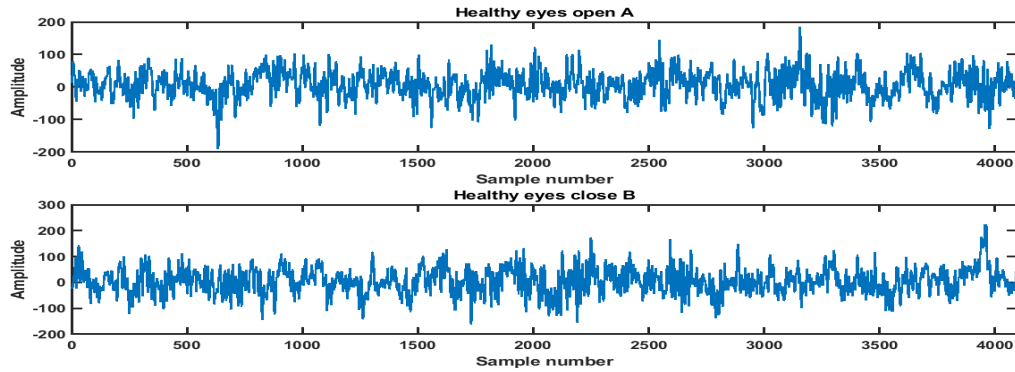


Fig. 2 Original healthy signals plotted in MATLAB, (A) eyes open (B) eyes close

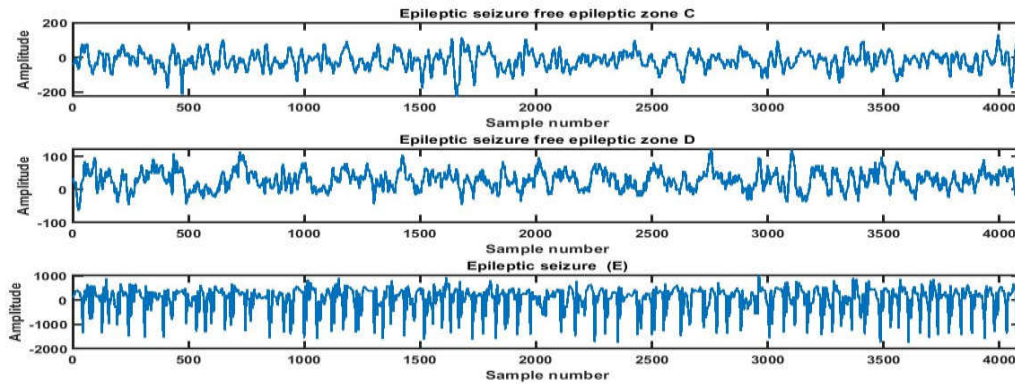


Fig. 3 Signals plotted in MATLAB, epileptic during seizure (E), and epileptic seizure free (C, D).

B. Denoising Of EEG Signal Based On Wavelet Transforms

The EEG signals that used in this study have a sampling frequency is 173.61 Hz, and thus the frequency range is 0–86.8 Hz. Therefore, we utilized filters that eliminate unnecessary frequencies and concentrate solely on the range corresponding to the five EEG rhythms that are medically recognized, specifically delta (0–4 Hz), theta (4–8 Hz), alpha (8–16 Hz), beta (16–32 Hz), and gamma (32–64 Hz). The wavelet transform is good tool used for analysis the EEG signal [14]. WT illustrates the signal

in the time frequency domain. Generally, a wavelet is defined as the following equation [15].

$$\psi_{s,t}(t) = |s|^{-\frac{1}{2}} \varphi\left\{\left(\frac{T-t}{s}\right)\right\} \quad (1)$$

where t and, $s \neq 0$, denotes the scale and translation parameters. In this study, we used symlet2, haar, and coiflet2 mother function for denoising of the EEG signal; Figure 4 showed the mother wavelet functions Plotted in MATLAB. The steps of denoising algorithms based on the wavelet transform are: (1) EEG Decomposition using the (DWT), (WPT), and (SWT), (2) Thresholding and (3) EEG Reconstruction using the inverse WT.

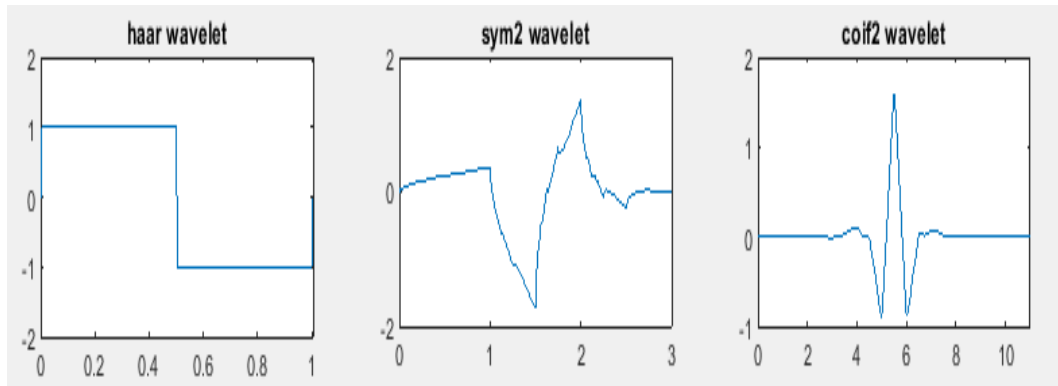


Fig. 4 Mother functions used for denoising signal in MATLAB.

DWT decomposes a discrete time signal $x[k]$ into two signals: Detail (D_j) and Approximation(A_j), described as: -

$$D_j[i] = \sum_z x[k].h[2.i - k] \quad (2)$$

$$A_j[i] = \sum_z x[k].i[2.i - k] \quad (3)$$

Choosing the proper number of wavelet decomposition levels (or scale levels) j_m is the first stage in the DWT decomposition. For the initial level, $j = 1$ signal $x[k]$ passes through both the high and low pass filter, $h[n]$ and $i[n]$ respectively, then the procedure of down-sampling by two [16], as illustrated in Figure 5 and denoising by using DWT is shown in Figure 6.

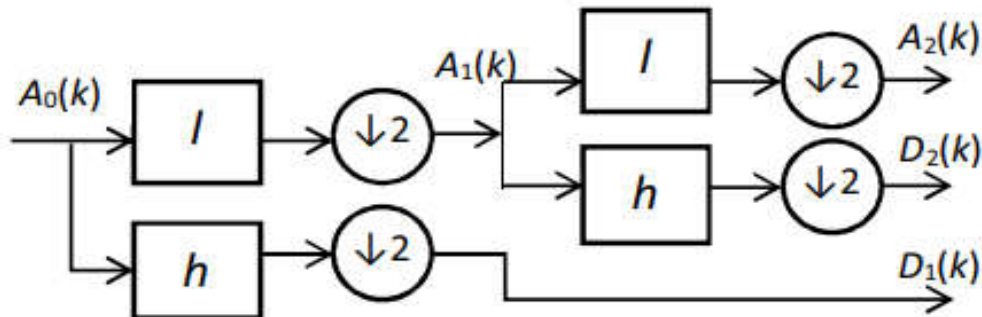


Fig. 5 DWT for scale level 2.

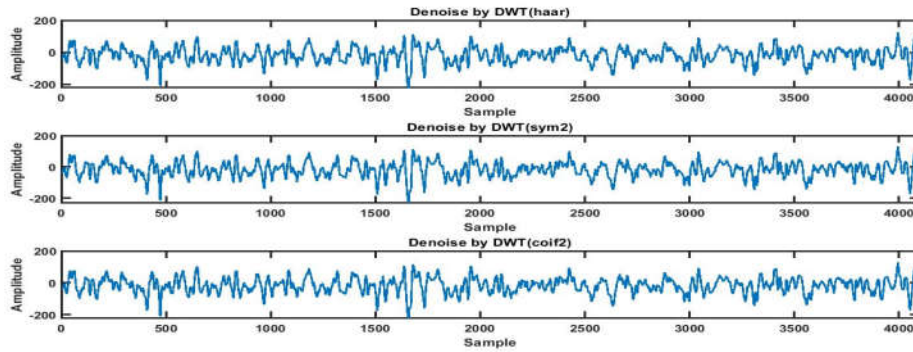


Fig. 6 Denoising by using DWT. (1) haar, (2) symlet2, (3) coiflet2

C. Wavelet Packet Transform

A development of the standard wavelet transform is the WPT (WPT). In the WPT, the detail coefficients are broken down at the initial level of decomposition, forming a structure referred to as the wavelet packet tree in literature [17]. This procedure is illustrated in Figure 7. As a result, the outcomes achieved possess superior resolution in both the time and frequency domains. The WPT of a signal $x(t)$ is defined in equation: -

$$x_p^{n,j} = 2^{-\frac{j}{2}} \int x(t) \mu_n(2^{-j}t - p) dt \quad (4)$$

The symbol j stands for the number of decomposition levels, also known as scale parameters; the symbol p stands for the position parameter; and the number n is the number of packets as a result of the decomposition process. $\mu(T)$ Is the function wavelet packet. The denoising outputs using WPT is shown in Figure 8.

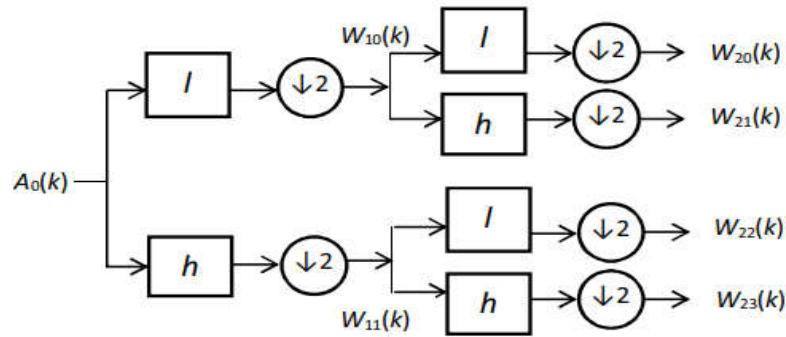


Fig. 7 WPT for scale level 2.

D. Stationary Wavelet Transform

While time invariance is important for statistical signal processing applications, DWT is affected by time variance. SWT overcomes the DWT's translation invariance problem. However, SWT is sluggish and contains duplicate data [18]. The

wavelet toolbox has been used in MATLAB for SWT. The denoising outputs using SWT is shown in Figure 9.

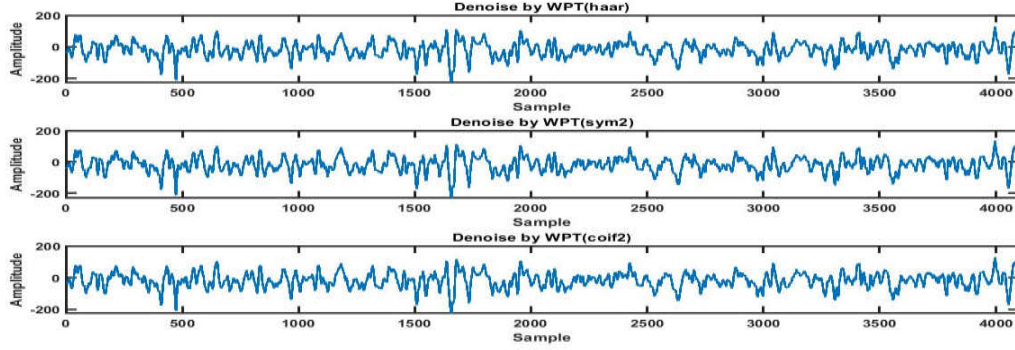


Fig. 8 WPT method. (1) haar, (2) symlet2, and (3) coiflet2.

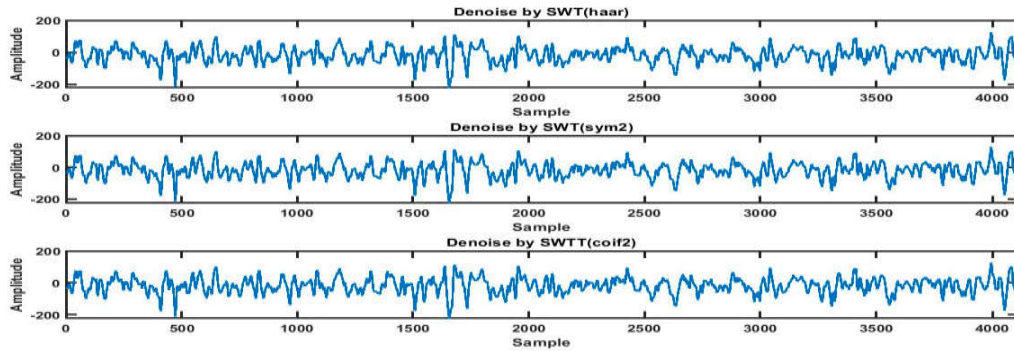


Fig. 9 SWT method. (1) haar, (2) symlet2, and (3) coiflet2.

E. Threshold

The primary concept of wavelet denoising is to achieve the perfect elements of the signal from the signal that has noise. This process demands the assessment of the degree of noise. There are many possible approaches to the estimation of the noise level [19]. In this study, we used the universal threshold technique for estimation noise because we applied different threshold techniques on random selected signal and this method gave better results. The threshold and noise estimates are computed using the WT factors.

Calculate the median and δ by

$$\sigma = \frac{\text{median}\{|c_0|, |c_1|, \dots, |c_{n-1}|\}}{0.6745} \quad (5)$$

where $|c_0|, |c_1|, \dots, |c_{(n-1)}|$ are the wavelet coefficients, and where the numerator is rescaled by 0.6745 in the denominator [20]. The threshold, τ , is calculated by

$$\text{Threshold}, t = \delta \sqrt{\ln N} \quad (6)$$

where δ is the estimated noise. N is the total number of samples for the EEG signal. The wavelet toolbox in MATLAB has been used for the threshold.

$$X_{HARD} = \begin{cases} X & \text{if } |X| > t \\ 0 & \text{if } |X| \leq t \end{cases} \quad (7)$$

$$X_{SOFT} = \begin{cases} |X| - t & \text{if } |X| > t \\ 0 & \text{if } |X| \leq t \end{cases} \quad (8)$$

F. EEG Signal Decomposition

The DWT has also been used for the decomposition of EEG signal, and this method was explained in the part EEG denoising. In this part will be discussed the other three methods used for the decomposition of EEG signal. The EEG signal decomposition outputs using DWT are shown in Figures 10 and 11.

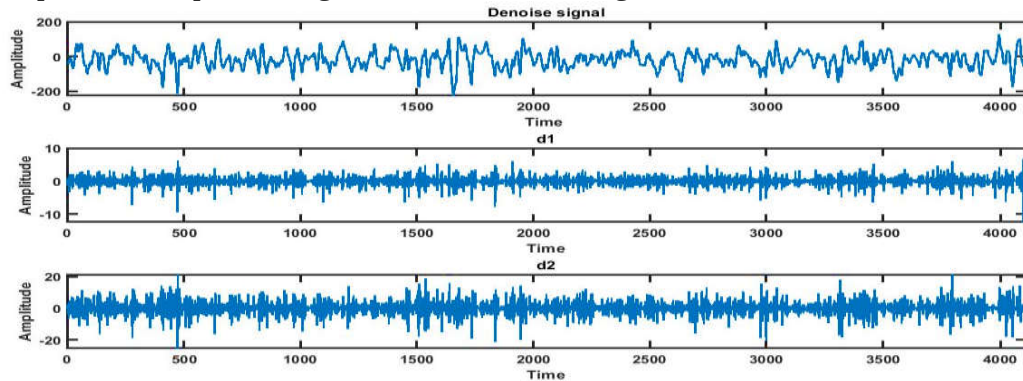


Fig. 10 DWT method. (1) denoised EEG signal by using SWT symlet2 for epileptic person seizure free, (2) detail1, (3) detail 2.

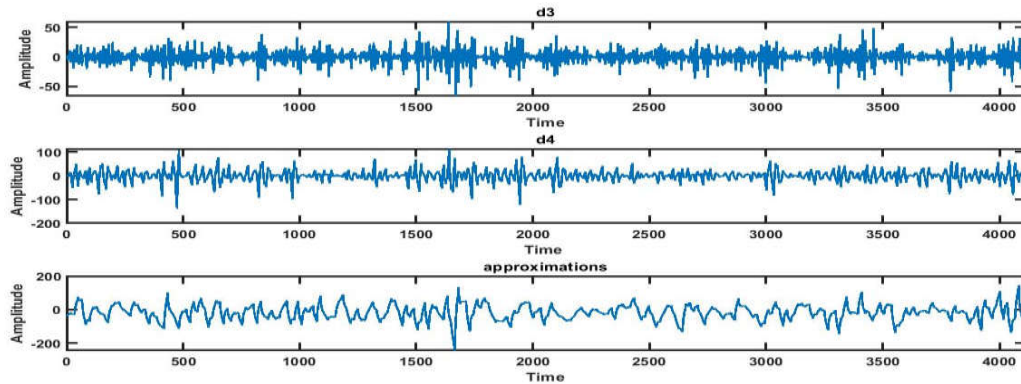


Fig. 11 DWT method. (1) Detail3, (2) detail4, and (3) approximation.

G. Maximal Overlap Discrete Wavelet Transform

Is similar to the DWT in that low-pass and high-pass filters are applied to the input signal at each level. The number of wavelet and scaling coefficients, however, is

equal to the number of sample observations at every step of the transform, and the MODWT does not decimate the coefficients. Put differently, the MODWT coefficients take into account the outcome of a basic modification made to the pyramid algorithm employed for computing DWT coefficients. This modification involves not down-sampling the output at every level and including zeros between the coefficients in the scaling and wavelet filters [10]. The EEG signal decomposition outputs using MODWT are shown in Figures 12 and 13.

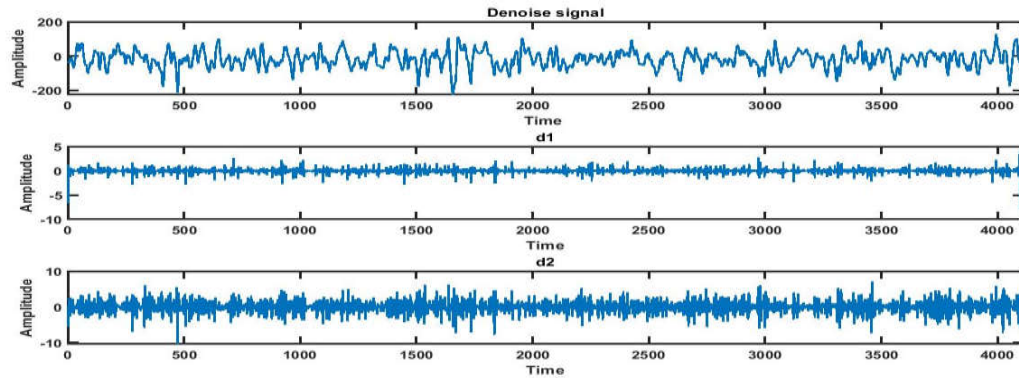


Fig. 12 MODWT method. (1) denoised EEG signal using the SWT symlet2 for epileptic person seizure free, (2) Detail1, (3) detail 2.

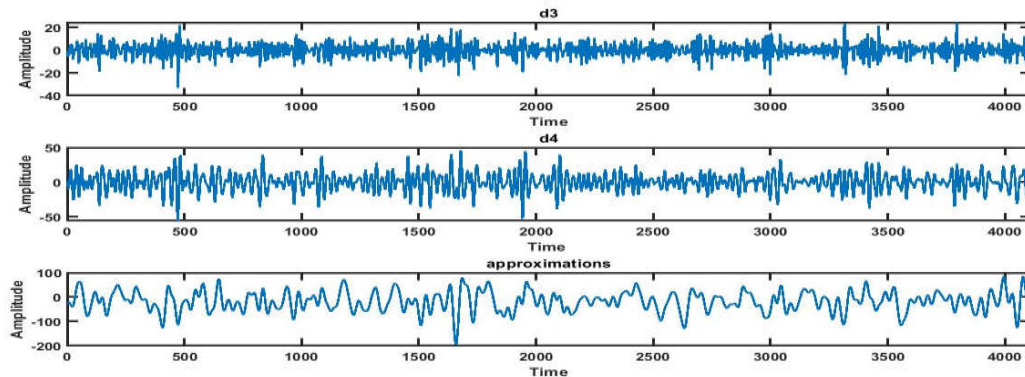


Fig. 13 MODWT method. (1) Detail3, (2) detail4, and (3) approximate.

H. Empirical Mode Decomposition

EMD technique examines signals that are not stationary and has gained widespread acceptance for the analysis of biological signals. This method decomposing a signal $x(t)$ into Intrinsic Mode Functions (IMFs) and residual. These IMFs should meet the following two conditions:

1. There can be no more than one difference in the number of extrema or zero crossings.
2. The average value of the envelopes formed by local maxima and local minima is zero at all times[21].

$$x = \sum_{j=1}^{j_m} c_j + r_A \quad (9)$$

where c_j is j^{th} IMF and r_A is the residue. The EEG signal decomposition outputs using EMD are shown in Figures 14 and 15.

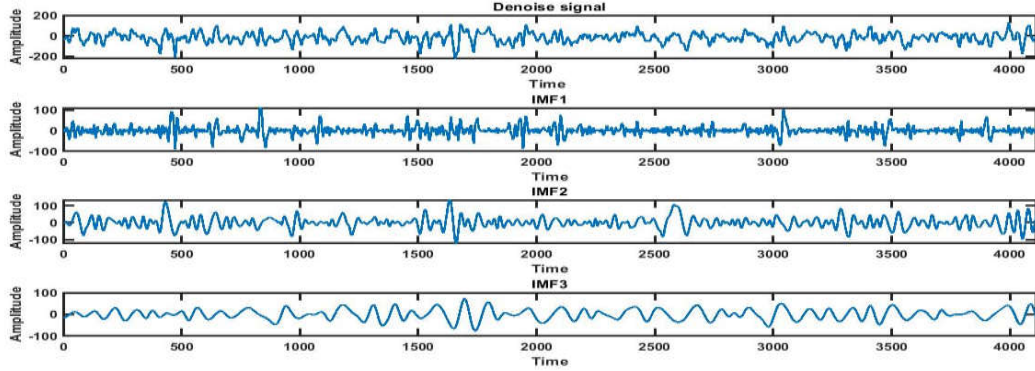


Fig. 14 EMD method. (1) denoised EEG signal by using SWT symlet2 for epileptic person seizure free, (2) IMF1, (3) IMF2, and (4) IMF3

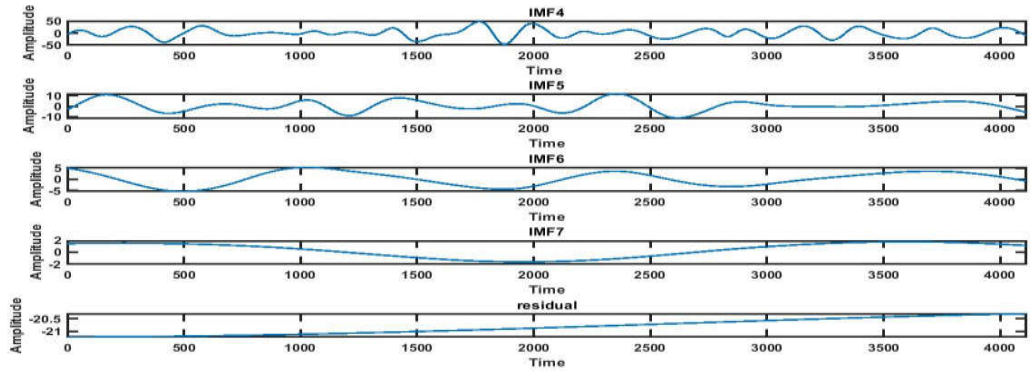


Fig. 15 EMD method (1) IMF4, (2) IMF5, (3) IMF6, (4) IMF7, and (5) residual

I. Variational Mode Decomposition

VMD is method for time frequency decomposition of EEG signals. The process of VMD is listed as follows [11]: 1. Obtain the unilateral frequency spectrum of each mode by computing the associated analytic signal by using the Hilbert transform (in which $j^2 = -1$):

$$\left(\delta(t) + \frac{j}{\pi t}\right) \times u_k(t) \quad (10)$$

2. By multiplying an exponential tuned with the expected center frequency, convert the frequency spectrum of each mode to baseband.:

$$\left[\left(\delta(t) + \frac{j}{\pi t}\right) \times u_k(t)\right] e^{-jw_k t} \quad (11)$$

3. Calculate the bandwidth of each mode by using the squared l^2 -norm of the gradient.

$$\left\| \partial(t) \left[\left(\delta(t) + \frac{j}{\pi t}\right) \times u_k(t)\right] e^{-jw_k t} \right\|_2^2 \quad (12)$$

The EEG signal decomposition outputs using VMD are shown in Figures 16 and 17.

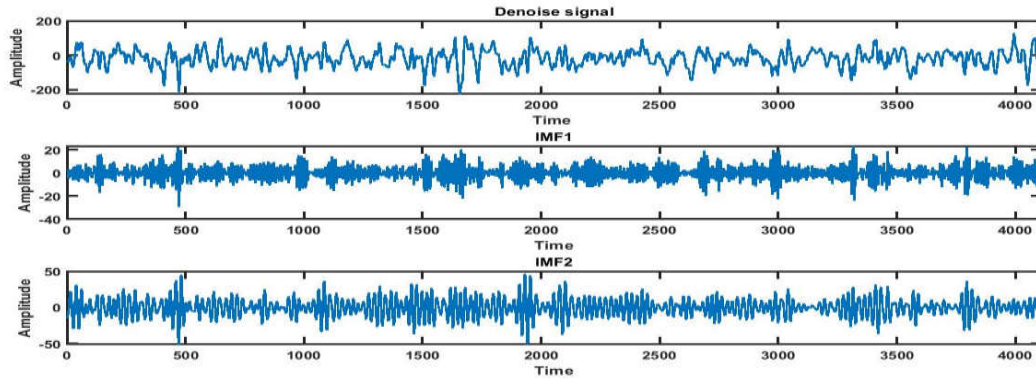


Fig. 16 VMD method. (1) denoised EEG signal using the SWT symlet2 for epileptic person seizure free, (2) IMF1, and (3) IMF2

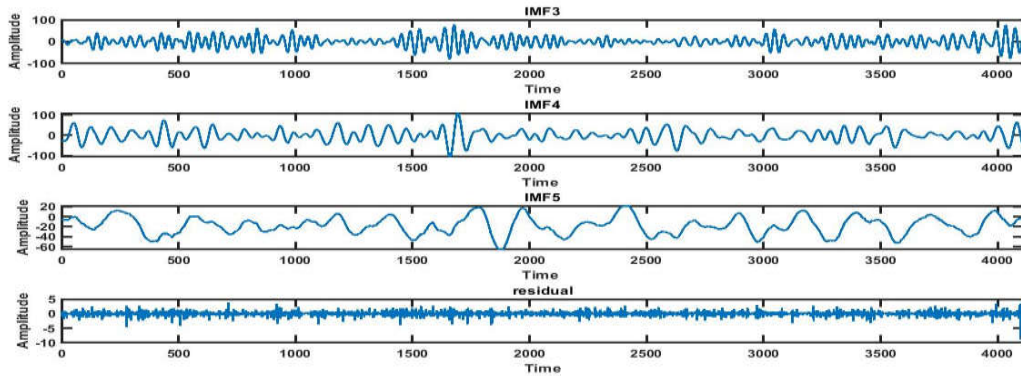


Fig. 17 VMD method. (1) IMF3, (2) IMF4, (3) IMF5, and (4) residual

3. RESULTS

Various performance metrics such as MSE, PSNR, and SNR are used to evaluate the best method used for denoise EEG signal. SNR suggests the artifact rejection functionality of a set of rules for any noisy signal, the SNR is typically expressed in terms of decibels, the higher the SNR value indicates that a filter is better [22]. If x shows authentic signal and x_1 shows signal after removing artifacts, then:

$$SNR = 10 \log_{10} \frac{x}{x-x_1} \quad (13)$$

The MSE, which measures how closely the denoise signal resembles the authentic signal, is described as the mean or average of the square of the distinction between the authentic and denoised signal. A filter is preferable if its value is lower [23]. MSE is described as:

$$MSE = \frac{1}{n} \sum_{i=1}^n (x - x_1)^2 \quad (14)$$

PSNR is an expression for the ratio between a signal's highest possible value (power) and the power of a noise source that distorts the signal and lowers the quality of its

representation, PSNR is usually expressed as a logarithmic quantity using the decibel scale. A filter that has a higher PSNR value is more effective [23]. PSNR is given as:

$$PSNR = 20 \log_{10} \frac{MAX(x)}{\sqrt{MSE}} \tag{15}$$

MAX(x) Is the maximum signal value that exists in signal with artifacts. Tables 1 to 3 shows the obtained performance measures for different conditions.

Table 1. SNR, PSNR, and MSE for DWT at different body conditions

Mother function	sets	A	B	C	D	E
	Parameters					
Haar	SNR	21.4802	22.8111	23.6227	21.8542	41.8816
	PSNR	34.3592	35.7386	36.3121	31.5154	53.1772
	MSE	13.2309	13.5053	11.9401	10.6726	14.9888
symlet2	SNR	21.9555	23.2114	24.7907	22.669	42.1068
	PSNR	34.9603	36.1389	37.694	32.3301	53.4025
	MSE	11.8595	12.3161	9.1245	8.847	14.2311
coiflet2	SNR	22.5283	23.6161	25.6416	23.0007	42.5305
	PSNR	35.4072	36.5436	38.331	32.6619	53.8261
	MSE	10.3941	11.2203	7.501	8.1964	12.9086

Table 2. SNR, PSNR, and MSE for WPT at different body conditions

Mother function	sets	A	B	C	D	E
	Parameters					
Haar	SNR	21.9005	23.2162	24.1449	22.2452	42.2192
	PSNR	34.7794	36.1437	36.9013	31.9064	53.5148
	MSE	12.0106	12.3025	10.5874	9.7538	13.8677
symlet2	SNR	22.4571	23.6626	25.2804	23.0509	42.3157
	PSNR	35.336	36.5901	38.157	32.7121	53.6113
	MSE	10.5658	11.1008	8.1515	8.1022	13.5631
coiflet2	SNR	23.1862	24.0247	26.1768	23.5853	42.5109
	PSNR	36.0651	36.9523	38.8661	33.2464	53.8065
	MSE	8.9329	10.2127	6.6314	7.1642	12.9669

Table 3. SNR, PSNR, and MSE for SWT at different body conditions

Mother function	sets	A	B	C	D	E
	Parameters					
Haar	SNR	23.6171	24.896	27.1995	24.081	44.9039
	PSNR	36.4898	37.835	39.8996	33.743	56.2107
	MSE	8.1008	8.3342	5.2271	6.2156	7.4544
symlet2	SNR	24.1258	25.2941	27.3189	24.1905	45.7613
	PSNR	36.9985	38.2331	40.019	33.8627	57.0681
	MSE	7.2055	7.6042	5.0853	6.0145	6.119
coiflet2	SNR	24.2198	25.1129	27.2572	24.1309	45.9033
	PSNR	37.0925	38.052	39.9573	33.8031	57.2101
	MSE	7.0512	7.9281	5.2581	6.3024	5.9221

Also, Various performance metrics such Energy, correlation (corrcoef), and distances between the power spectral densities (PSD) are used to evaluate the best method used to decompose the EEG signal [24]. These metrics were calculated for each sub -bands from DWT, MODWT, EMD, and VMD. The energies of all IMF are determined in Eq. (16).

$$E_{IMFi} = \sum_{n=0}^{N-1} |IMFi[n]|^2, i = 1, 2, \dots, l. \tag{16}$$

The correlation coefficient(corrcoef) is a methodology used to indicate the relationship between two signals, and the (corrcoef) of all IMF is obtained, as demonstrated in Eq. (17).

$$\rho_{x, IMF_i} = \frac{C_{x, IMF_i}}{\sigma_x \sigma_{IMF_i}} \tag{17}$$

Here, C_{x, IMF_i} is the crosscovariance of the authentic signal and i th IMF, σ_x, σ_{IMF_i} are the standard deviations, and ρ denotes the (corrcoef). Every other selection approach, primarily based on (PSD) become also used by the usage of the (PSD) of the authentic signal and IMFs. The energy contained within the signal as a characteristic of frequency, per unit frequency, is described through the (PSD) of the signal. The Kullback Liebler distance (KLD) method is used to calculated distances between PSDs, is a type of statistical distance that measures how one possibility distribution isn't the same as a 2nd reference possibility distribution, as proven in Eq. (18)

$$dis_{KLD}(x, IMF_i) = \sum_{n=0}^{N-1} \log \frac{S_x(w_k)}{S_{IMF_i}(w_k)}, w_k = \frac{2\pi}{N} K \tag{18}$$

Here $S_x(.)$ is the power spectrum of the authentic signal, $S_{IMF_i}(.)$ is the power spectrum of the IMF, the $dis_{KLD}(x, IMF_i)$ illustrates the KLD between $S_x(.)$ and $S_{IMF_i}(.)$. Tables 4 to 7 shows the obtained performance measures for different conditions.

Table 4 . Calculated corrcoef, psd distance, energy for DWT (symlet2) at different body conditions

coefficient	sets	A	B	C	D	E
	Parameters					
detail1	psddistance	0.09	0.1349	0.0608	0.1837	0.0197
	energy	4.79E+04	6.37E+04	7.08E+03	4.74E+03	8.91E+06
	corrcoef	0.0829	0.0801	0.0271	0.0384	0.0977
detail2	psddistance	0.4742	0.4682	0.5086	0.4582	0.5577
	energy	3.29E+05	4.72E+05	6.69E+04	3.19E+04	7.77E+07
	corrcoef	0.2173	0.2187	0.0831	0.1004	0.2886
detail3	psddistance	0.4978	0.5724	0.4203	0.3876	0.5396
	energy	1.21E+06	1.83E+06	4.27E+05	1.38E+05	2.66E+08
	corrcoef	0.4171	0.4305	0.2102	0.2081	0.5343
detail4	psd distance	0.3747	0.4835	0.3289	0.3883	0.5055
	energy	1.83E+06	2.29E+06	1.88E+06	3.18E+05	1.91E+08
	corrcoef	0.5142	0.4802	0.4412	0.3158	0.452
approx	psd distance	0.0424	0.0185	0.0245	0.0012	0.1907
	energy	3.74E+06	5.35E+06	8.59E+06	6.04E+06	3.99E+08
	corrcoef	0.7137	0.7276	0.8681	0.9193	0.6459

Table 5. Calculated corrcoef, psd distance, energy for MODWT (symlet2) at different body conditions

coefficient	sets	A	B	C	D	E
	Parameters					
detail1	psd distance	2.3452	2.489	4.3018	2.703	5.4989
	energy	8.59E+03	1.63E+04	1.02E+03	1.29E+03	8.61E+05
	corrcoef	0.1885	0.1675	0.0731	0.0753	0.3037
detail2	psd distance	2.2042	2.2778	3.1751	2.0445	2.6913
	energy	1.08E+05	1.34E+05	1.32E+04	9.24E+03	2.13E+07
	corrcoef	0.3861	0.3972	0.1872	0.1823	0.5438
detail3	psd distance	1.3424	1.2981	2.0828	1.3692	0.847
	energy	6.13E+05	9.50E+05	1.36E+05	5.65E+04	1.57E+08
	corrcoef	0.6187	0.6322	0.3675	0.3183	0.701
detail4	psd distance	1.291	1.2805	1.5436	1.4288	1.3722
	energy	8.17E+05	1.08E+06	7.19E+05	1.50E+05	9.12E+07
	corrcoef	0.6913	0.6682	0.6168	0.4961	0.7174
approximate	psd distance	0.0338	0.0216	0.0232	2.00E-04	0.2567
	energy	3.51E+06	5.03E+06	8.06E+06	5.86E+06	3.15E+08
	corrcoef	0.7629	0.752	0.9341	0.9436	0.6934

Table 6. Calculated corrcoef, psd distance, energy for VMD at different body conditions

IMF(n)	sets	A	B	C	D	E
	Parameters					
IMF1	psd distance	0.3202	0.1261	0.3575	0.3633	0.319
	energy	1.49E+05	2.64E+05	1.54E+05	6.71E+04	2.53E+07
	corrcoef	0.2083	0.2212	0.1918	0.2127	0.247
IMF2	psd distance	0.3563	0.156	0.3023	0.409	0.2779
	energy	2.33E+05	1.46E+06	6.92E+05	1.57E+05	1.20E+08
	corrcoef	0.2969	0.4908	0.3849	0.3337	0.4866
IMF3	psd distance	0.097	0.2591	0.257	0.2733	0.2558
	energy	1.61E+06	1.42E+06	1.96E+06	4.95E+05	1.46E+08
	corrcoef	0.5688	0.508	0.6096	0.5407	0.5388
IMF4	psd distance	0.2474	0.3923	0.2249	0.2452	0.3585
	energy	1.35E+06	1.17E+06	3.07E+06	1.02E+06	1.11E+08
	corrcoef	0.5779	0.5016	0.7319	0.7514	0.5224
IMF5	psd distance	0.0544	0.0803	0.0395	0.0024	0.165
	energy	2.56E+06	3.66E+06	2.50E+06	3.89E+06	3.19E+08
	corrcoef	0.6569	0.674	0.5171	0.6066	0.6643
Residual	psd distance	2.0931	1.9103	5.5063	3.676	5.1793
	energy	5.89E+03	1.42E+04	2.42E+03	2.59E+03	1.44E+06
	corrcoef	0.1612	0.1292	0.123	0.1171	0.1623

Table 7. Calculated corrcoef, psd distance, energy for EMD at different body conditions

IMF(n)	sets	A	B	C	D	E
	Parameters					
IMF1	psddistance	0.3032	0.2207	1.4316	1.5733	0.1321
	energy	2.52E+06	3.98E+06	1.86E+06	2.84E+05	5.09E+08
	corrcoef	0.5664	0.5807	0.4682	0.2765	0.6281
IMF2	psddistance	0.2675	0.4372	0.4989	1.0369	-0.1435
	energy	1.96E+06	1.77E+06	4.24E+06	8.47E+05	4.43E+08
	corrcoef	0.4992	0.3463	0.6453	0.497	0.577
IMF3	psddistance	0.1971	0.1939	-0.0041	0.3027	0.1294
	energy	1.31E+06	2.14E+06	2.35E+06	9.98E+05	1.47E+08
	corrcoef	0.3537	0.4186	0.4795	0.5695	0.3079
IMF4	psddistance	0.0787	0.1019	-0.1286	0.2676	-1.0035
	energy	1.04E+06	1.69E+06	1.23E+06	9.43E+05	4.75E+07
	corrcoef	0.3843	0.3757	0.3317	0.523	0.0905
IMF5	psddistance	0.2459	-0.2614	1.4917	0.0707	-0.4614
	energy	5.56E+05	1.63E+06	9.42E+04	2.41E+05	6.84E+06
	corrcoef	0.2677	0.3089	0.1027	0.2007	0.0281
IMF6	psddistance	0.3342	0.0329	0.9268	-1.2596	0.5281
	energy	1.17E+05	1.72E+05	3.74E+04	6.00E+04	1.96E+06
	corrcoef	0.1431	0.0426	0.043	0.0157	0.0132
IMF7	psddistance	0.5073	0.04	4.0657	5.966	0.2705
	energy	3.79E+04	1.07E+05	6.16E+03	4.00E+03	1.13E+06
	corrcoef	-0.0015	0.0415	0.0158	-0.0106	0.0078
IMF8	psddistance	0.4004	0.7533	NA	6.0852	0.0965
	energy	4.33E+04	4.19E+04	NA	1.81E+03	1.95E+06
	corrcoef	-0.0139	0.0603	NA	0.0134	0.008
Residual	psddistance	-0.6535	1.112	-0.311	0.0404	0.834
	energy	3.83E+05	7.35E+04	1.78E+06	3.22E+06	4.31E+06
	corrcoef	-0.0197	-0.0417	0.0027	0.014	-7.00E-04

4. DISCUSSIONS

According to the scenarios and approaches described in the methodology, the results were as follows. In scenario one for the denoising step when applied DWT with level four on all data sets and used different mother functions, Haar, Symlet2, and coiflet2, the result has been presented in figure 6 for set (C), and recorded the values of SNR, PSNR, and MSE for all five sets in Table 1 for evaluated. In scenario two, when applied WPT also with level four on all data sets with three mother functions, haar, Symlet2, and coiflet2, the result has been presented in figure 8 for set (C), and recorded the values of SNR, PSNR, and MSE for all five sets in Table 2.

In scenario three, when applied SWT with three mother functions, haar, Symlet2, and coiflet2, on all data set with level four, the result has been presented in figure 9 for set (C), and recorded the values of SNR, PSNR, and MSE for all five sets in Table 3. The result showed that the highest value of SNR and PSNR in set (A) and set

(E) when using *coiflet2* stationary wavelet level four and the lowest value of MSE was found in these cases, while in set (B) and sets (C and D), the result showed that the highest value of SNR and PSNR and the lowest value of MSE when using *symlet2* stationary wavelet level four compared with *coiflet2* stationary wavelet level four.

The result of approach one for the decomposition step has been shown in figures 10 and 11 respectively, for set (C) when applied DWT with level four, and the values of energy, correlation, and distances between the PSDs for all five sets were recorded in Table 4. The result of approach two has been shown in figures 12 and 13, respectively, in set (C) when applied maximal overlap DWT with level four, and the values of energy, correlation, and distances between the PSDs for all five sets were recorded in Table 5.

Also, the result of approach three has been shown in Figures 14 and 15, respectively, in set (C) when applied EMD, and the values of energy, correlation, and distances between the power spectral densities (PSD) for all five sets were recorded in Table 6. Finally, the result of approach four has been shown in Figures 16 and 17, respectively, in set (C) when applied VMD, and the values of energy, correlation, and distances between the power spectral densities (PSD) for all five sets were recorded in Table 7.

The result showed the highest value of energy of IMF1 in set (E) when used EMD compared with other methods, and the lowest value of the distances between PSD showed in IMF6 also when used EMD for epileptic in t set (D) compared with other methods, but the highest value of correlation showed in approximate of maximal overlap DWTs for epileptic in the set (D) compared with other methods.

5. CONCLUSIONS

Research is always striving to improve denoising and decomposition techniques for EEG signals to make the diagnosis of epileptic seizures more accurate and faster. In this study, the efficiency of nine filters, DWT, WPT, and SWT, with three mother functions, Haar, Symlet2, and *coiflet2* have been evaluated and compared by using three parameters such as SNR, PSNR, MSE, and the result showed that the *symlet2* SWT level four is the best method used for signal denoising. Then the efficiency of four decomposition methods, DWT, MODWT, EMD, and VMD have been compared and evaluated by using three parameters (Energy, correlation coefficient, distances between the PSD, and the result showed that the EMD is the best method used for signal decomposition. It is recommended to use other mother functions of the wavelet transform for denoising and decomposition of EEG signals and applied to the same data set that has been used. Also, it is recommended to apply this method to other data sets related to seizures and comparing results with results has been obtained in this study.

Funding Statement: The authors received no specific funding for this study.

Conflicts of Interest: The authors declare that they have no conflicts of interest to report regarding the present study.

REFERENCES

- [1]. G.L. Wallstrom, R.E. Kass, A. Miller, J.F. Cohn and N.A. Fox, "Automatic correction of ocular artifacts in the EEG: A comparison of regression-based and component-based methods," *International Journal of Psychophysiology* , vol. 53, no. 2, 2004, pp. 105-119.
- [2]. I.I Goncharova, D.J McFarland, T.M Vaughan and J.R Wolpaw, "EMG contamination of EEG: Spectral and topographical characteristics," *Clinical Neurophysiology*, vol. 114, no. 9, 2003, pp. 1580-1593.
- [3]. A.Q. Hamal and W.A. Rehman, "Artifact Processing of Epileptic EEG Signals: An Overview of Different Types of Artifacts," *International Conference on Advanced Computer Science Applications and Technologies*, 2013, pp. 358-361.
- [4]. R. Princy, P. Thamarai and B. Karthik, "Denoising EEG Signal Using Wavelet Transform," *International Journal of Advanced Research in computer Engineering & Technology* , vol. 4, no. 3, 2015, pp. 1-8.
- [5]. P. Khatwani and A. Tiwari, "A survey on different noise removal techniques of EEG signals," *International Journal of Advanced Research in Computer and Communication Engineering*, vol. 2, no. 2, 2013, pp. 1091-1095.
- [6]. Md. Mamun, M. Al-Kadi and M. Marufuzzaman, "Effectiveness of Wavelet Denoising on Electroencephalogram Signals", *Journal of Applied Research and Technology*, vol. 11, no. 1, 2013, pp.156-160.
- [7]. V. Singh and R. Sharma, "Wavelet Based Method for Denoising of Electroencephalogram," *International Journal of Advanced Research in Computer Science and Software Engineering*, vol. 5, no. 4, 2015, pp. 1-10.
- [8]. D. Sinha and K. Thangavel, "Performance Analysis of wavelet Thresholding for Denoising EEG Signal," *Journal of Computer Sciences and Engineering*, vol. 6, no. 4, 2018, pp. 214-218.
- [9]. Harender and R.K. Sharma, "EEG Signal Denoising based on Wavelet Transform," *International Conference on Electronics, Communication and Aerospace Technology*, pp. 758-761, 2017.
- [10]. A.A.A. Dghais and M.T. Ismail, "A Comparative Study between Discrete Wavelet Transform and Maximal Overlap Discrete Wavelet Transform for Testing Stationarity," *International Journal of Mathematical Science and Engineering*, vol. 7, no. 12, 2013, pp. 1-10.
- [11]. A. Pradhan, "A Survey of Classification of EEG signals using EMD and VMD for Epileptic Seizure Detection," *International Journal of Engineering Research &Technology*, vol. 9, no. 5, 2020, pp. 495-498.
- [12]. E.A. Mohamed, M. ZukiYusoff, A.S. Malik, M.R. Bahloul, D.M. Adam and I.K. Adam, "Comparison of EEG signal decomposition methods in classification of motor-imagery BCI", *Springer Science*, vol.77, 2018, pp. 21305–21327.
- [13]. R.G. Andrzejak, K. Lehnertz, F. Mormann, C. Rieke, P. David and C.E. Elger, "Indications of nonlinear deterministic and finite-dimensional structures in time series of brain electrical activity," *Department of Epileptology, University of Bonn*, 2001.
- [14]. G. Inuso, F.L. Foresta, N. Mammone and F.C. Morabito, "Brain activity investigation by EEG processing: Wavelet analysis, kurtosis and Renyi's entropy for artifact detection," *International Conference on Information Acquisition*, 2007, pp. 195-200.

- [15]. O.A. Rosso, M.T. Martin, A. Figliola, K. Keller and A. Plastino, "EEG analysis using wavelet-based information tools," *Journal of Neuroscience Methods*, vol.153, no. 2, 2006, pp.163-182.
- [16]. P. Ghorbanian, D.M. Devilbiss, A.J. Son, A. Bernstein, T. Hessand H. Ashrafiuon, "Discrete Wavelet Transform EEG Features of Alzheimer's Disease in Activated States", *Annual International Conference of the IEEE Engineering in Medicine and Biology Society*, 2012, pp. 2937-2940.
- [17]. M. Varanis, J.M. Balthazar, A. Silva, A.G. Mereles and R. Pederiva, "Remarks on the Sommerfeld effectcharacterization in the wavelet domain," *Journal of Vibration and Control*, vol. 25, no. 1, 2019, pp.98-108.
- [18]. P. Senthil Kumar, R. Arumuganathan, K. Sivakumar and C. Vimal, "An adaptive method to remove ocular artifacts from EEG signals using wavelet transform," *Journal of Applied Sciences Research*, vol. 5, no.7, 2009, pp. 741-745.
- [19]. B. Ergen, "Comparison of Wavelet Types and Thresholding Methodson Wavelet Based Denoising of Heart Sounds," *Journal of Signal and Information Processing*, vol. 4, no. 3, 2013, pp .164-167.
- [20]. R. Mahajan and B.I. Morshed , "Unsupervised Eye Blink Artifact Denoising of EEG Data with Modified Multiscale Sample Entropy, Kurtosis, and Wavelet-ICA," *IEEE journal of biomedical and health informatics*, vol. 19, no. 1, 2015, pp. 158-165.
- [21]. J. Kevric and A. Subasi, "Comparison of signal decomposition methods in classification of EEG signals for motor-imagery BCI system," *Biomedical Signal Processing and Control*, vol. 31, 2017, pp. 398-406.
- [22]. M.H. Soomro, N. Badruddin, M.Z. Yusoff and A.S. Malik, "A method for automatic removal of eye blink artifacts from EEG based on EMD-ICA," *IEEE 9th International Colloquium on Signal Processing and its Applications*, 2013, pp. 129-134.
- [23]. M.T. Akhtar, W. Mitsuhashi and C.J. James, "Employing spatially constrained ICA and wavelet denoising, for automatic removal of artifacts from multichannel EEG data," *Signal Processing*, vol. 92, no. 2, 2012, pp. 401-416.
- [24]. O.K. Cura, S.K. Atli, H.S. Türe and A. Akan, "Epileptic seizure classifications using empirical mode decomposition and its derivative," *BioMedical Engineering OnLine*, vol. 10, 2020, pp. 1-22.